

Comparing Macrorheology and One- and Two-Point Microrheology in Wormlike Micelle Solutions

M. Buchanan,^{*,†,§,⊥} M. Atakhorrami,^{†,§} J. F. Palierne,[‡] and C. F. Schmidt[†]

Department of Physics and Astronomy, Vrije Universiteit Amsterdam, de Boelelaan 1081, Amsterdam, The Netherlands, and Laboratoire de Physique, Ecole Normale Supérieure de Lyon, Lyon, France

Received January 17, 2005; Revised Manuscript Received August 11, 2005

ABSTRACT: We present here a comparison between three rheological techniques to verify a recently developed optical microrheology technique. As a model viscoelastic fluid we have used wormlike micelle solutions which are well-characterized Maxwell fluids. Using the same samples, we have measured the viscoelastic response function using macroscopic rheology as well as one-particle and two-particle microrheology. With all three techniques we have obtained frequency-dependent complex shear moduli over large and overlapping frequency ranges. Excellent agreement of the results from all three techniques was observed. This was expected given that characteristic length scales of the solution, such as persistence length and mesh size, were significantly smaller than the probe particle size. Our results provide a much needed quantitative verification of microrheology on a simple model system.

Introduction

The shear elastic properties of viscoelastic materials, such as polymer or colloidal solutions, are commonly measured by mechanical rheometers. Storage and loss moduli of a material can be measured by application of strain while measuring stress or vice versa, and probe geometries of order centimeters are typically used. Recently developed optical microrheology techniques, in contrast, use micron-sized particles that are embedded in the material to obtain the viscoelastic response parameters.¹ In contrast to macroscopic mechanical rheology techniques, there is no strain applied to the material during the measurement. This is particularly useful in complex fluids where even small imposed strains can cause a structural reorganization of the material and change its viscoelastic properties.

Response parameters can be measured either by actively manipulating the probe particles with magnetic fields or with light (optical traps)² or in a passive mode by merely recording the thermal fluctuations of the particles. Various methods have been utilized to measure the displacement fluctuations of the embedded particles. Video tracking or “rheological microscopy” has been applied to a variety of polymer systems such as λ -DNA solutions³ as well as to biological cells.⁴ The highest frequency that can be measured using this technique is half the video frequency (Nyquist frequency), typically 25 or 30 Hz. Higher bandwidths can be reached using diffusing wave spectroscopy (DWS)^{5,6} or optical trapping techniques combined with laser interferometry with fast photodiodes to track individual particles.^{7,8}

The complex shear modulus of the embedding medium can be calculated from the Brownian motion of the particle using results from linear response theory.⁹ In the linear response regime, the fluctuation–dissipa-

tion theorem relates position fluctuations to the imaginary part of the response function. A Kramers–Kronig integral then makes it possible to calculate the real part of the response function. Generalized Stokes–Einstein relationships, which differ for the one-particle and the two-particle method, can then be used to extract the complex shear modulus.^{8,10} Data analysis has also been performed in a different way, using a Laplace transform of the mean-square displacement and then employing a fitting procedure assuming the analytic form of the storage and loss elastic modulus.^{5,11,12} Here we use the first method to obtain the viscoelastic modulus directly from the data, avoiding any fitting procedures.

In general, microrheology is a useful tool to probe spatially resolved viscoelastic properties of inhomogeneous materials, and it can be applied to study small samples, such as biological cells. Furthermore, the technique has a bandwidth of up to megahertz, much larger than conventional macrorheology, and it is sensitive enough to measure low elastic moduli (<1 Pa) that are not accessible to macrorheometers. Passive microrheology is ideally suited to investigate materials that respond nonlinearly to low strains, such as many biopolymer systems.

Since microrheology techniques are relatively new and have been applied initially to samples such as actin solutions or cells which are problematic in macrorheology, there is still a need to rigorously determine under what conditions one can expect to measure the same bulk shear moduli as measured by conventional rheometers. A number of possible effects can lead to differing results, which at the same time opens up new and interesting possibilities to characterize materials on a microscopic scale. One possibility is that the probe particle locally perturbs its environment on the same scale that it probes, e.g., by causing local depletion or enrichment of the medium.¹³ This is expected to occur if there are characteristic length scales in the sample that are on the order of or larger than the probe size. Nonstick boundary conditions on the surface of the probes would also affect the results.¹⁴ Furthermore, if the sample is a polymer solution, compressional or free

* Corresponding author: e-mail cfs@nat.vu.nl.

[†] Vrije Universiteit Amsterdam.

[‡] Ecole Normale Supérieure de Lyon.

[§] Both authors contributed equally to this work.

[⊥] Current address: Physics of Geological Processes, Department of Physics, University of Oslo, Norway.

draining modes should in principle be measurable since there is no constant-volume constraint. The fluctuation–dissipation theorem which is used in the passive modes might not be applicable in nonequilibrium or glassy systems. Local perturbation effects can be circumvented and at the same time quantified by measuring the correlated fluctuations of pairs of probe particles, a method termed two-particle microrheology.^{13,15,16} Evidence for depletion effects has been reported in λ -DNA solutions where a difference between one- and two-particle results was observed.³

To date there has been no clear quantitative comparison of microrheology with macrorheology on a well-characterized system. This has been due to the limited overlap over the frequency range between the two techniques. Typical commercial rheometers measure up to a maximum frequency of about 10 Hz. At such low frequencies microrheology tends to give quite noisy results. Furthermore, there is also a limit in the range of elastic moduli one can measure with both techniques: Microrheology performs well in soft systems but gets less accurate from ~ 100 Pa upward, while macrorheology is often not very accurate below 10 Pa. Microrheology to date has been extensively used on biopolymer solutions, such as actin networks or cells, for which macrorheology has been notoriously inaccurate¹⁷ or impossible.

We report here on rheology experiments with a simple and well-studied model system, namely a surfactant forming wormlike micelles in solution. The objective of this paper is to quantitatively compare the results of both one- and two-particle microrheology and macrorheology with the same samples. Technical details of the two-particle microrheology technique will be published elsewhere.¹⁸ The wormlike micelle solutions, made from cetylpyridinium chloride and sodium salicylate in 0.5 M sodium chloride brine, exhibit dynamics similar to polymer solutions; however, the breakage dynamics ensure a single relaxation time in the slow dynamics.^{19,20} This results in very simple and well-understood rheological properties, namely Maxwell behavior at low frequencies.²¹ Furthermore, for this sample one-particle microrheology should not be sensitive to depletion or other probe particle effects, since the relevant length scales such as mesh size and persistence length are smaller than the particle size. We expect therefore agreement between all three techniques.

Experimental Methods

Materials. Wormlike micelles were prepared from the surfactant cetylpyridinium chloride (CPyCl) dissolved in brine (0.5 M NaCl) with sodium salicylate (NaSal) as strongly binding counterions. All samples had a molar ratio Sal/CPy = 0.5. Samples were made in batches of 50 mL and equilibrated and stored at ambient (controlled) lab temperature of 21.5–22.0 °C. The microrheology experiments were performed in the same lab at the same temperature. The wormlike micelles have a typical diameter of 2–3 nm, lengths between 100 nm and 1 μ m, and a persistence length of order 10 nm.²⁰ Experiments were performed with micelle concentrations between 0.5 and 4 wt %, i.e., in the semidilute regime ($c > c^*$, $c^* \sim 0.3$ wt %) where micelles are entangled. The average mesh size varies between 30 and 10 nm for c between 1 and 5 wt %.²⁰

Macrorheology. A custom-designed piezo-rheometer²² was used to measure directly the loss and storage shear elastic moduli of the samples. The sample was contained between two glass plates mounted on piezoelectric ceramics. One of the plates was made to oscillate vertically with an amplitude of about 1 nm by applying a sine wave to the ceramic. This

movement induces a squeezing flow in the sample and stress transmitted to the second plate is measured by the other piezoelectric element. The strain is extremely small ($\gamma < 10^{-4}$) so the sample structure was likely not altered by the flow. The setup allows us to measure the storage ($G'(\omega)$) and loss ($G''(\omega)$) shear modulus for frequencies ranging from 0.1 Hz to 10 kHz. All experiments were done at 21.8 °C except for $c_p = 4$, which was done at 22.4 °C. The setup was hermetically sealed to avoid evaporation.

One-Particle Microrheology (1PMR). All experiments were performed using a custom-built optical microscope equipped with an optical trap and a laser-interferometric position detection system as described previously.⁸ Briefly, an infrared laser ($\lambda = 1064$ nm, ND:YVO₄, Compass, Coherent, Santa Clara, CA) was focused into the sample via a microscope objective lens (Zeiss Neofluar, 100 \times , oil immersion, NA: 1.3) to optically trap a particle in the sample. The back-focal plane of the condenser collecting the laser light downstream of the trap was imaged onto a special-design PN photodiode operated at a reverse bias voltage of 100 V (YAG444-4A, Perkin-Elmer, Vaudreuil, Canada) to avoid high-frequency attenuation.²³ Displacement fluctuations of the trapped particle in the plane normal to the optical axis were recorded on a PC using Labview (National Instruments, Austin, TX) after analog signal conditioning and A/D conversion with sample frequencies up to 195 kHz.⁸ The lab temperature was stabilized to 21.4 ± 1 °C.

The particles used in the experiments were silica beads of diameter 0.98 μ m (Bangs Laboratories, Fisher, IN) and 1.16 μ m (Van't Hoff Laboratory, Utrecht University, Utrecht, Netherlands) for single- and two-point microrheology experiments, respectively. A small quantity (below 10^{-3} vol %) was added to each sample before measurements, and the sample was then introduced into the sample chamber. The sample chamber consisted of a glass slide and coverslip connected by two strips of double-stick tape (about 75 μ m thick) and was sealed after loading the sample with grease (Apiezon L) at the open ends. After a bead was trapped, all measurements were performed at a distance of about 20 μ m from the bottom surface of the sample chamber. The instrument was aligned before each set of experiments, and among other criteria, it was tested that x and y autocorrelation spectra of beads trapped in pure solvent were overlapping. The shear that the solution is exposed to when filling the chamber transiently changes the structure of the sample. To ensure that the samples were completely relaxed and isotropic after the filling procedure and after the probe particle was positioned with the help of the optical trap, particle fluctuations in the directions parallel (x) with and perpendicular (y) to the long axis of the chamber were compared. Averaged autocorrelation spectra of 60 s segments of data typically differed right after filling the chambers, with the x -spectra (in the flow direction) typically showing a higher rms amplitude of motion than the y -spectra, but slowly converged over 5–15 min. After complete relaxation, between 8 and 16 data sets were recorded for each sample, using different beads (minimum of three) in different locations of the sample. Data were taken at two different sampling rates, 20 and 195 kHz. At 20 kHz sample rate, the laser power was set low (3–5 mW) to avoid a large effect of the optical trap on the particle fluctuations; at 195 kHz laser power had to be set somewhat higher (15–30 mW) to avoid shot noise at the high-frequency end of the spectrum.

Calibration factors are needed to convert the amplified quadrant diode signals to actual displacements in nanometers. These factors were determined from displacement autocorrelation spectra in water of particles from the same batch as used in the micelle experiments. Autocorrelation spectra of particles trapped in a purely viscous fluid have a Lorentzian shape, and from the amplitude of the Lorentzian at high frequencies, calibration factors can be determined if particle size, solvent viscosity, and temperature are used as (given) parameters.²⁴ Three or more particles in water were trapped again 20 μ m from the glass surface at both the low and high laser power used in the micelle experiments, and their displacement fluctuations were recorded at sampling rates of

20 and 195 kHz. The variance of the results was around 5%, which is mainly due to particle polydispersity.

Two-Particle Microrheology (2PMR). A pair of focused laser beams with wavelengths $\lambda = 830$ nm (diode laser, CW, IQ1C140, Laser 2000) and $\lambda = 1064$ nm (NdVO₄, see above) (power less than 10 mW, measured before coupling into the microscope) was used to weakly trap a pair of silica particles far away from other particles, at several separation distances r between 3 and 20 μm . The x and y position fluctuations of each trapped particles were detected with a pair of quadrant photodiodes, the $\lambda = 1064$ nm laser was detected as described above, and for the $\lambda = 830$ nm we used a standard silicon-type PN photodiode with a reverse bias voltage of 15V (10 mm diameter, Spot9-DMI, UDT, Hawthorne, CA).

Data Evaluation. We processed the recorded position fluctuation data off-line to obtain the viscoelastic moduli in a similar manner for both the 1PMR and the 2PMR method.

Within linear response a (complex) single- or interparticle response function $\alpha_{kl}^{(ij)}(\omega)$ relates the displacement of each particle in x or y direction $u_k^{(i)}(\omega)$ to the force $F_k^{(i)}(\omega)$ applied to the same particle or to the other one; $u_k^{(i)}(\omega) = \alpha_{kl}^{(ij)}(\omega) \times F_l^{(j)}(\omega)$, written in Fourier space, where $i, j = 1, 2$ are particles labels, $k, l = x, y$ are coordinate directions, and $\omega = 2\pi f$ is the radial frequency. For example, $\alpha_{xx}^{(1,1)}(\omega)$ is the single-particle response function relating the x displacement of particle 1 to the force acting on particle 1 in x direction, or $\alpha_{xx}^{(1,2)}(\omega)$ is the interparticle response function relating the x displacement of particle 1 to the force applied to particle 2 in x direction.

For 1PMR we calculate the Fourier transform of the displacement autocorrelation $S_k^{(i)}$ of each particle from the recorded position fluctuations $u_k^{(i)}(t)$:

$$S_k^{(i)} = \int \langle u_k^{(i)}(t) u_k^{(i)}(0) \rangle e^{i\omega t} dt \quad (1)$$

in all experiments reported here the medium was homogeneous. Thus, we calculate an averaged $S_{\text{auto}} = 1/4 \langle S_x^1 + S_y^1 + S_x^2 + S_y^2 \rangle$.

We chose the coordinate system such that the x -axis is parallel to the line connecting the centers of the two particles and the y -axis perpendicular to that.

For 2PMR we calculate the Fourier transforms of the two displacement cross-correlations that are nonzero to first order:

$$S_{\parallel}(\omega) = \int \langle u_x^{(1)}(t) u_x^{(2)}(0) \rangle e^{i\omega t} dt \quad (\text{parallel to center line}) \quad (2a)$$

$$S_{\perp}(\omega) = \int \langle u_y^{(1)}(t) u_y^{(2)}(0) \rangle e^{i\omega t} dt \quad (\text{perpendicular to center line}) \quad (2b)$$

From these correlation functions we first obtain the imaginary parts of the complex response functions $\alpha_{\text{auto}}(\omega) = \alpha'_{\text{auto}}(\omega) + i\alpha''_{\text{auto}}(\omega)$ and $\alpha_{\parallel\perp}(\omega) = \alpha'_{\parallel\perp}(\omega) + i\alpha''_{\parallel\perp}(\omega)$, which, in thermal equilibrium and in the absence of external forces, are related to the correlation functions by the fluctuation–dissipation theorem:⁹

$$\alpha''_{\text{auto}}(\omega) = \frac{\omega}{2k_B T} S_{\text{auto}}(\omega) \quad \text{and} \quad \alpha''_{\parallel\perp}(\omega) = \frac{\omega}{2k_B T} S_{\parallel\perp}(\omega) \quad (3)$$

where $k_B T$ is the thermal energy.

The real parts of the response functions are then computed by a Kramers–Kronig integral over the imaginary parts:

$$\alpha'_{\text{auto}} = \frac{2}{\pi} \int_0^\infty \frac{\zeta \alpha''_{\text{auto}}(\omega)}{\omega^2 + \zeta^2} d\zeta \quad \text{and} \quad \alpha'_{\parallel\perp} = \frac{2}{\pi} \int_0^\infty \frac{\zeta \alpha''_{\parallel\perp}(\omega)}{\omega^2 + \zeta^2} d\zeta \quad (4)$$

In principle, there is a systematic error expected for α' due to the finite integration limits in the KK integral.⁸ This error is here generally negligible when we sample at 195 kHz. Since

the error is in α' , it will be more apparent in samples with large G' . In the data presented here, the maximum $G_0 = 10$ Pa where we can still neglect the effect. However, for stiffer samples a small error will arise in α' .

So far we have calculated response properties of the particles. These are determined by the viscoelastic properties of the embedding medium via generalized Stokes–Einstein relationships:^{8,15}

$$\alpha_{\text{auto}}(\omega) = \frac{1}{6\pi R G(\omega)}, \quad \alpha_{\parallel}(\omega) = \frac{1}{4\pi r G(\omega)}, \quad \text{and} \quad \alpha_{\perp}(\omega) = \frac{1}{8\pi r G(\omega)} \quad (5)$$

where $G(\omega)$ is the complex shear modulus, R is the particle radius, and r is the separation distance between the two particles. While both the parallel and the perpendicular interparticle response can be used to determine $G(\omega)$ in 2PMR, we find experimentally that the perpendicular channel is noisier than the parallel one. Furthermore, at higher frequencies solvent inertia becomes visible, and the effect is larger on the perpendicular channel.²⁵ We thus present in the following the data measured by the parallel interparticle response function as the 2PMR results.

The optical traps limit the Brownian motion of the particles and have an effect on the storage modulus calculated from the fluctuation data if not corrected for.²⁶ The response functions $\alpha'(\omega)$ and $\alpha''(\omega)$ were corrected for the trap effect before calculating $G(\omega)$ as described elsewhere.²⁶ For the lower sampling rate (20 kHz, laser power ≤ 5 mW) the trap effect was negligible for all micelle concentrations except for 0.5 wt %, where the correction amounted to decrease of $G'(\omega)$ of 50% at 5 Hz up to less than 1% at 1 kHz. Heating of the samples in the trap focus is negligible because of the low laser power.²⁷

Results and Discussion

Figure 1 shows a comparison of complex shear moduli measured with mechanical macrorheology and with microrheology. $G'(\omega)$ and $G''(\omega)$ curves are shifted vertically for clarity. Surfactant concentrations were $c_p = 0.5, 1, 2$, and 4 wt %. 2PMR and 1PMR data were taken simultaneously as described above, averaging over x and y fluctuations of both particles (four independent data sets) over a total recording time of 200–300 s gives relatively smooth curves for 1PMR. In 2PMR curves are clearly more noisy because there is just one independent data set for each recording (parallel direction), and the amplitude of the cross-correlation is smaller than the amplitude of the autocorrelation and decays as $1/r$.

With increasing micelle concentration storage and loss moduli show a trend expected for an increasingly elastic polymer network.²⁸ There is disagreement between macro- and microrheology data at frequencies < 1 Hz (panels B and D). This is most likely due to small errors in the trap correction, which becomes dominant at the lowest frequencies in $G'(\omega)$.

Agreement between all three techniques quantitatively validates the new microrheology methods. It is theoretically expected when certain criteria are met. First, the micelle solution must be homogeneous on the scale of the particle size. Second, the particle should not perturb the local environment in which it moves on a scale comparable to its own size. When the particle size is much larger than any network length scale such as the mesh size or the polymer persistence length, as is the case here, this criterion will be met. In semiflexible polymer systems this is not the case, and discrepancies have been found between 1PMR and 2PMR.^{29,30} Third, there should be a nonslip boundary condition between

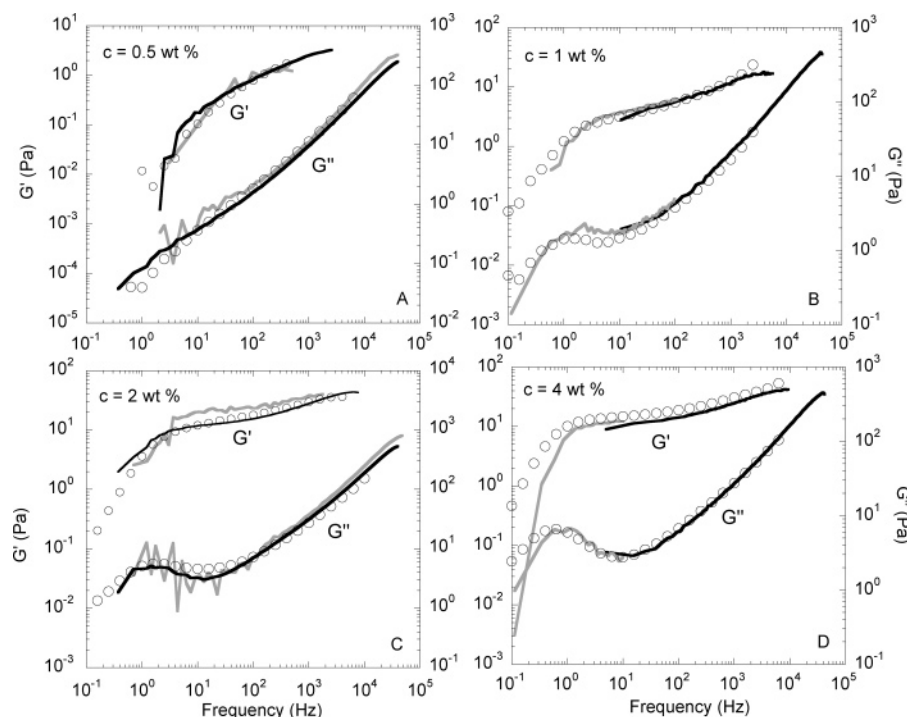


Figure 1. Loss modulus (right axes) and elastic modulus (left axes) for four surfactant concentrations 0.5 (A), 1 (B), 2 (C), and (D) 4 wt % are plotted as a function of frequency. Curves are in (A) and (C): macro-rheology (circles), 1PMR (black lines), and 2PMR (gray lines) in 0.5 and 2 wt %; in (B) and (D): 1PMR with 20 kHz sampling rate (gray line) and 1PMR with 195 kHz sampling rate (black lines). All microrheology data were logarithmically binned with the factor of 1.2 relating the widths of successive bins.

the micelles and the particle surface. Particularly at elevated frequencies viscous coupling is expected to ensure nonslip boundary conditions. Our results demonstrate that for the wormlike micelle solutions studied all criteria were satisfied. In particular, the good agreement between one- and two-particle microrheology demonstrates that local perturbations around the probes such as depletion, enrichment, or slip boundary conditions did not occur to a measurable degree. Our results here are in contrast to what has been claimed for polystyrene solutions.³¹

In 2PMR one expects a minimal distance between two particles where approximation of a homogeneous medium and a Stokes flow field would cease to be valid. The distance which this corresponds to is the larger of either particle size or internal length scales of the system. Here we did not observe any deviations from $1/r$ scaling in 2PMR results down to a distance of $4\ \mu\text{m}$, for the $D = 1.16\ \mu\text{m}$ particles.³²

Previous work using diffusing wave spectroscopy (DWS) had found agreement between that implementation of microrheology and conventional macro-rheology in polymer and emulsion systems at low frequencies.^{5,6} However, the range of comparison was severely restricted ($<20\ \text{Hz}$) due to the limitations of the mechanical rheology.

Conclusions

We have verified that there is excellent agreement between mechanical rheology probing a sample at macroscopic scales and one- and two particle microrheology experiments up to high frequencies. With a piezo-actuated mechanical rheometer we could extend the range for comparison to 10 kHz, much above what has been achievable with commercial rheometers. The system chosen for the comparison, wormlike micelles in

high salt concentrations, has strongly screened electrostatic interactions and structural length scales much smaller than the particle size. We have shown here that in such a system microrheology, and in particular the relatively simple one-particle technique, is sufficient to probe the bulk rheological properties of the medium. These results should now make it possible to use the advantages of microrheology, such as small sample size, high bandwidth, and high sensitivity, to quantitatively study a variety of systems.

Acknowledgment. We thank J. F. Berret, M. E. Cates, P. Bartlett, L. Starrs, F. C. MacKintosh, and A. Levine for helpful discussions and E. Peterman, J. van Mameren, and G. Koenderink for technical help. This work was supported by the Foundation for Fundamental Research on Matter (FOM).

References and Notes

- (1) MacKintosh, F. C.; Schmidt, C. F. *Curr. Opin. Colloid Interface Sci.* **1999**, *4*, 300–307.
- (2) Ashkin, A. *Proc. Natl. Acad. Sci. U.S.A.* **1997**, *94*, 4853–4860.
- (3) Chen, D. T.; Weeks, E. R.; Crocker, J. C.; Islam, M. F.; Verma, R.; Gruber, J.; Levine, A. J.; Lubensky, T. C.; Yodh, A. G. *Phys. Rev. Lett.* **2003**, *90*.
- (4) Rehage, H.; Hoffmann, H. *J. Phys. Chem.* **1988**, *92*, 4712–4719.
- (5) Mason, T. G.; Weitz, D. A. *Phys. Rev. Lett.* **1995**, *75*, 2770–2773.
- (6) Cardinaux, F.; Cipolletti, L.; Scheffold, F.; Schurtenberger, P. *Europhys. Lett.* **2002**, *57*, 738–744.
- (7) Mason, T. G.; Ganesan, K.; Zanten, J. H. v.; Wirtz, D.; Kuo, S. C. *Phys. Rev. Lett.* **1997**, *79*, 3282–3285.
- (8) Schnurr, B.; Gittes, F.; MacKintosh, F. C.; Schmidt, C. F. *Macromolecules* **1997**, *30*, 7781–7792.
- (9) Landau, L. D.; Lifshitz, E. M.; Pitaevskii, L. P. *Statistical Physics*; Pergamon Press: Oxford, 1980.
- (10) Chaikin, P. M.; Lubensky, T. *Principles of Condensed Matter*; Cambridge University Press: Cambridge, 1994.

- (11) Mason, T. G. *Rheol. Acta* **2000**, *39*, 371–378.
- (12) Bird, R. B.; Armstrong, R. C.; Hassager, O. *Dynamics of Polymeric Liquids*; John Wiley and Sons: New York, 1977.
- (13) Crocker, J. C.; Valentine, M. T.; Weeks, E. R.; Gisler, T.; Kaplan, P. D.; Yodh, A. G.; Weitz, D. A. *Phys. Rev. Lett.* **2000**, *85*, 888–891.
- (14) Starrs, L.; Bartlett, P. *Faraday Discuss.* **2003**, *123*, 323–334.
- (15) Levine, A. J.; Lubensky, T. C. *Phys. Rev. Lett.* **2000**, *85*, 1774–1777.
- (16) Levine, A. J.; Lubensky, T. C. *Phys. Rev. E* **2002**, *65*.
- (17) Xu, J.; Palmer, A.; Wirtz, D. *Macromolecules* **1998**, *31*, 6486–6492.
- (18) Atakhorrami, M.; et al., not published.
- (19) Walker, L. M. *Curr. Opin. Colloid Interface Sci.* **2001**, *6*, 451–456.
- (20) Berret, J. F.; Appell, J.; Porte, G. *Langmuir* **1993**, *9*, 2851–2854.
- (21) Ferry, J. D. *Viscoelastic Properties of Polymers*, 3rd ed.; Wiley: New York, 1980.
- (22) Hebraud, P.; Lequeux, F.; Palierne, A. J. *Langmuir* **2000**, *16*, 8296–8299.
- (23) Peterman, E. J. G.; van Dijk, M. A.; Kapitein, L. C.; Schmidt, C. F. *Rev. Sci. Instrum.* **2003**, *74*, 3246–3249.
- (24) Gittes, F.; Schmidt, C. F. In *Methods in Cell Biology*; Academic Press: 1998; Vol. 55, pp 129–156.
- (25) Atakhorrami, M.; Koenderink, G. H.; Schmidt, C. F.; MacKintosh, A. F. C., submitted to *Phys. Rev. Lett.*
- (26) Atakhorrami, M.; Kwiecinska, J.; Addas, K. M.; Koenderink, G. H.; Levine, A.; MacKintosh, F. C.; Schmidt, A. C. F., to be submitted.
- (27) Peterman, E. J. G.; Gittes, F.; Schmidt, C. F. *Biophys. J.* **2003**, *84*, 1308–1316.
- (28) Buchanan, M.; Atakhorrami, M.; Palierne, J. F.; MacKintosh, F. C.; Schmidt, C. F. *Phys. Rev. E* **2005**, *72*, 011504.
- (29) Gardel, M. L.; Valentine, M. T.; Crocker, J. C.; Bausch, A. R.; Weitz, D. A. *Phys. Rev. Lett.* **2003**, *91*, 158302.
- (30) Koenderink, G. H.; Atakhorrami, M.; MacKintosh, F. C.; Schmidt, C. F., submitted to *Phys. Rev. Lett.*
- (31) Starrs, L.; Bartlett, P. *J. Phys.: Condens. Matter* **2003**, *15*, S251–S256.
- (32) Atakhorrami, M.; Schmidt, C. F., submitted to *Rheol. Acta*.

MA0500990